




Restoration of quantized Thouless pumping in non-Hermitian systems

Mingyuan Gao (高铭远),¹ Chong Sheng (盛冲)^{1,*} Kun Ding (丁鲲)^{2,†}
Shining Zhu (祝世宁)¹ and Hui Liu (刘辉)^{1,‡}

¹*National Laboratory of Solid State Microstructures and School of Physics,
Collaborative Innovation Center of Advanced Microstructures,
Nanjing University, Nanjing, Jiangsu 210093, China*

²*Department of Physics, State Key Laboratory of Surface Physics,
and Key Laboratory of Micro and Nano Photonic Structures (Ministry of Education),
Fudan University, Shanghai 200438, China*



(Received 5 August 2025; revised 28 September 2025; accepted 10 October 2025; published 27 October 2025)

Thouless pumping manifests as a quantized transport phenomenon in time-driven Hermitian systems, protected by topological invariants. Non-Hermitian physics, arising in open systems, significantly affects the topological properties of quantum systems, giving rise to an intriguing interplay between topology and non-Hermiticity. We study Thouless pumping in generic non-Hermitian systems using the tight-binding formalism, and demonstrate that the transport dynamics of topological pumping are qualitatively distinct from those in Hermitian systems. Specifically, the Thouless pumping is governed by the interplay between the complex Berry curvature and the complex energy spectrum, deviating from the conventional quantized Chern number. Notably, we found that the deviation can be eliminated when system's average imaginary spectrum vanishes, restoring the charge pumping to Chern number in non-Hermitian systems. We validate our analytical findings through concrete examples. Our work provides new insights into transport phenomena in non-Hermitian experimental setups, such as lossy on-chip photonic systems.

DOI: [10.1103/3jcd-dz3f](https://doi.org/10.1103/3jcd-dz3f)

I. INTRODUCTION

Topological charge pumping, a dynamic phenomenon extensively studied in one-dimensional (1D) Hermitian systems and dubbed as Thouless pumping [1,2], exhibits quantized charge transport under adiabatic periodic modulations. The charge displacement per cycle is determined by the Berry curvature on a synthetic two-dimensional (2D) manifold of momentum and time, corresponding to the Chern number. Recent theoretical advances have extended Thouless pumping to non-Abelian generalizations [3–5], higher dimensional [6], nonlinear interaction [7–9], and the fractional pumping across multiple bands [10]. These advancements have been experimentally realized in various platforms, such as ultracold atoms [11–13], acoustic systems [5], and photonic devices [14,15]. However, the ubiquity of system-environment interactions poses significant challenges for these experimental realizations. Non-Hermitian theory has emerged as a powerful framework for describing open quantum systems, motivating further exploration of Thouless pumping under non-Hermitian dynamics. For example, the Ref. [16] has established a general framework of biorthogonal Thouless pumping in non-Hermitian systems. Nevertheless, the dynamics of physical observables in such systems remains largely unexplored.

Non-Hermiticity has revolutionized the understanding of topology in quantum systems [17–24], extending the en-

ergy spectrum into the complex domain and enriching topological structures from wave functions to spectra. And it has given rise to diverse phenomena, including the generalized bulk-edge correspondence [25–28], biorthogonal Berry curvature, point-gap topology, and the energy winding number [23]. Notably, non-Hermiticity induces nonunitary dynamics, fundamentally altering the behavior of wavefunctions [29–31]. Examples include non-Bloch quenching [32], edge bursts [33,34], and the asymmetric transport caused by the non-Hermitian skin effect (NHSE) [35–37]. Recent work by Ref. [35] has identified a dynamical signature of the NHSE in real space, revealing a profound connection between the energy spectrum area under periodic boundary condition (PBC) and the early-time acceleration of wave packets. While this previous study focused solely on the influence the energy spectrum topology on the center-of-mass evolution of wavepacket, it is evident that non-Hermiticity also modifies the wave-function topology. This raises a compelling question: How do the simultaneous effects of the wave-function topology and the energy spectral topology influence the evolution of observable physical quantities?

In this work, we generalize the Thouless pumping to generic 1D non-Hermitian systems by incorporating the effects of both wavefunction topology and energy spectrum topology. Our approach parallels Hermitian Thouless pumping (TP), focusing on the expectation values of the position operator defined on the evolved right eigenstates. However, following such way will bring various difficulties, considering that it violates the nature of biorthogonal formation in non-Hermitian regime [16]. For instance, since the evolution operators in non-Hermitian systems are

*Contact author: csheng@nju.edu.cn

†Contact author: kundong@fudan.edu.cn

‡Contact author: liuhui@nju.edu.cn

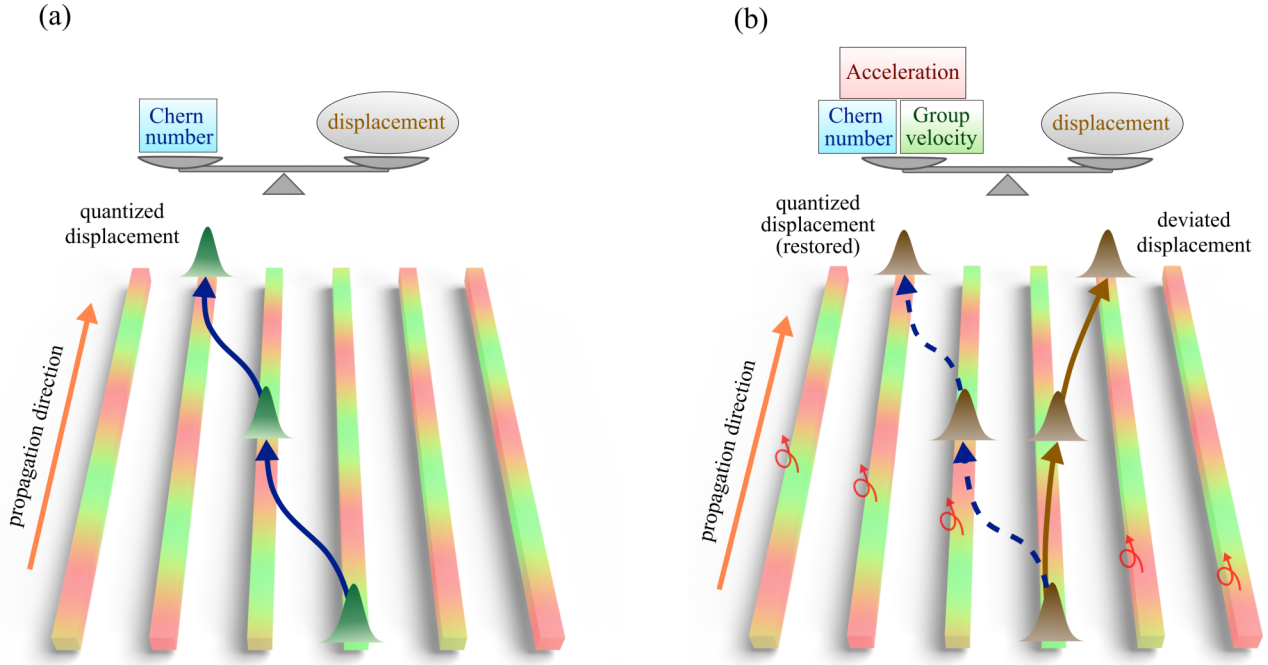


FIG. 1. The schematic of Thouless pumping in 1D non-Hermitian system, compared to the Hermitian case (a) Hermitian Thouless pumping and (b) Non-Hermitian Thouless pumping.

generally nonunitary, normalization of the evolved wavefunction is not preserved, which necessitate renormalization for the expectation value of position. Additionally, Wannier states constructed from a non-Hermitian Hamiltonian involve superpositions of right eigenstates within a single band, where interference between eigenstates is unavoidable due to the lack of orthonormality among right eigenstates. To address this, we introduce a Berry curvature defined on both right and left eigenstates, naturally incorporating the imaginary part of the non-Hermitian Berry curvature. Our results demonstrate that non-Hermitian charge pumping arises from the combined contributions of Hermitian and non-Hermitian Berry curvatures, group velocities, and complex energy spectra. The findings reveal that non-Hermiticity generally deviates charge pumping from the quantized Chern number, stemming from the interplay between complex Berry curvature and complex energy spectra. While such deviation might appear as a natural consequence of non-Hermiticity, we further investigate the sufficient conditions required to eliminate the deviation while retaining non-Hermiticity. Based on our analytical formula, we propose two criteria to restore the quantized charge pumping, which involve specific requirements on the complex band structure and the profile of the Berry curvature. Furthermore, we find that in pseudo-Hermitian systems, these conditions are naturally satisfied, enabling the restoration of charge pumping back to the Chern number for both topologically trivial and non-trivial cases.

This work is organized as follows. In Sec. II, we derive Thouless pumping in a generic tight-binding non-Hermitian model. In Sec. III, we demonstrate a nonreciprocal model to uncover the physical origins of non-Hermitian Thouless pumping. In Sec. IV, we establish the criteria under which Thouless pumping in non-Hermitian systems restores the quantized transport predicted by the Chern number. Finally, we summarize our findings in Sec. V.

II. THEORY

In 1D time-dependent Hermitian systems, Thouless pumping arises when specific modulations induce a nontrivial Chern number, establishing a precise correspondence between the topological Chern number and the quantized charge transport [Fig. 1(a)]. In this section, we extend the discussion to the non-Hermitian regime and investigate the general evolution formula of wave-packet's mass center.

A. Non-Hermiticity with Bloch formation

Non-Hermiticity poses significant challenges in exploring the interplay between topological properties and dynamical evolution. While recent studies have explored topological phases in non-Hermitian systems, they typically rely on similarity transformations that map non-Hermitian Hamiltonians to Hermitian counterparts [27,28]. However, such transformations are generally not tractable for arbitrary non-Hermitian systems, especially those with complex shapes of generalized Brillouin zones (GBZs). Extending the wave vector k into the complex wavevector $\beta(k) = k + i\mu(k)$, as required by non-Bloch theory, often results in ill-defined Fourier bases and Wannier states. For instance, the Fourier basis in GBZ is expressed as using tight-binding formulations:

$$|\beta\rangle = \frac{1}{\sqrt{N}} \sum_n e^{-ikn + \mu(k)n} |n\rangle, \\ \langle\beta^L| = \frac{1}{\sqrt{N}} \sum_n e^{ikn - \mu(k)n} \langle n|. \quad (1)$$

It is evident that the orthogonality condition $\langle\beta^L|\beta\rangle \neq \delta_{\beta,\beta'}$ is violated when $\mu(k)$ depends on k . Wannier states, defined as $|w(n)\rangle \propto \sum_k |u_k\rangle |\beta(k)\rangle$, are delocalized under the non-Bloch formalism due to the NHSE, where $|u_k\rangle$ represents

the eigenstate in momentum space. Notably, the non-Bloch framework is also incompatible with the dynamic quantities, such as observables like the mass center of wave-packet, $\langle \psi_k^R | \hat{x} | \psi_k^R \rangle$, which are defined solely on the evolved right eigenvector $|\psi_k^R\rangle$. These quantities are analytically challenging to analyze within the GBZ and the non-Bloch Fourier basis. Therefore, we retain the conventional Bloch framework for our investigation.

B. Berry curvature as the imaginary part of quantum geometry tensor

In Hermitian systems, the Berry curvature, defined on the synthetic two-dimensional Brillouin zone, plays a fundamental role in Thouless pumping. Specially, the Berry curvature directly determines the Chern number, which quantifies the average displacement of eigenstates within the corresponding energy band. Moreover, the Berry curvature is closely related to the quantum geometry tensor (QGT) [38–40]. And QGT in Hermitian systems is expressed by

$$\begin{aligned}\chi_{mn} &= \langle \partial_m \psi | \partial_n \psi \rangle - \langle \partial_m \psi | \psi \rangle \langle \psi | \partial_n \psi \rangle \\ &= \langle \partial_m \psi | \partial_n \psi \rangle - A_m A_n.\end{aligned}\quad (2)$$

where the Berry connection is given by $A_m = i\langle \psi | \partial_m \psi \rangle$, and the ψ is the instantons eigenstate. Usually, the Berry curvature corresponds to the imaginary and antisymmetric part of the QGT as

$$B_{mn} = i(\chi_{mn} - \chi_{nm}) = \partial_m A_n - \partial_n A_m, \quad (3)$$

while the real part of the QGT defines the quantum metric,

$$g_{mn} = \text{Re}[\chi_{mn}] = \frac{1}{2}(\chi_{mn} + \chi_{nm}). \quad (4)$$

In Hermitian systems, the quantum metric is symmetric, and the Berry curvature is purely real. However, in non-Hermitian systems, the quantum metric acquires an anti-symmetric component, leading to a complex Berry curvature. The non-Hermitian QGT is conventionally defined as [39,41]

$$\chi_{mn}^{LR} = \langle \partial_m \psi^L | \partial_n \psi^R \rangle - \langle \partial_m \psi^L | \psi^R \rangle \langle \psi^L | \partial_n \psi^R \rangle. \quad (5)$$

and the quantum metric is expressed as the real part of the QGT.

$$\begin{aligned}g_{mn}^{LR} &= \text{Re}[\chi_{mn}^{LR}] = \frac{1}{2}(\langle \partial_m \psi^L | \partial_n \psi^R \rangle + \langle \partial_n \psi^R | \partial_m \psi^L \rangle \\ &\quad - A_m^{LR} A_n^{LR} - A_n^{LR} A_m^{LR})\end{aligned}\quad (6)$$

where the non-Hermitian Berry connection is $A_m^{LR} = i\langle \psi^L | \partial_m \psi^R \rangle$. The imaginary part of the Berry curvature $B_{mn}^{LR} = \partial_m A_n^{LR} - \partial_n A_m^{LR}$ corresponds to the antisymmetric part of the quantum metric as

$$\text{Im}[B_{mn}^{LR}] = g_{mn}^{LR} - g_{nm}^{LR} = \frac{1}{2}(\chi_{mn}^{LR} + \chi_{nm}^{RL} - \chi_{nm}^{LR} - \chi_{mn}^{RL}), \quad (7)$$

while the imaginary part of the Berry curvature does not directly contribute to the non-Hermitian Chern number, our study demonstrates that the antisymmetric part of the quantum metric significantly influences the dynamical processes in non-Hermitian Thouless pumping. Specifically, it plays a crucial role in the observed deviation of the pumping displacement from the quantized Chern number.

C. General non-Hermitian model

We consider a one-dimensional non-Hermitian system defined on an arbitrary Hilbert space. To illustrate our theory, we employ a tight-binding model with a finite lattice, where the Hamiltonian is expressed by

$$H(t) = \sum_{n=0}^{N-1} \sum_{m=-l}^l \sum_{\alpha, \beta} H_{n+m, \alpha, n, \beta}(t) |n+m, \alpha\rangle \langle n, \beta|, \quad (8)$$

where the state vector $|n, \alpha\rangle = |n\rangle \otimes |\alpha\rangle$ represents a state localized in the n -th unit cell and sublattice α . The parameter m denotes the inter-cell coupling index, and $H_{n+m, \alpha, n, \beta}$ represents the real-space matrix element of the Hamiltonian. The lattice includes couplings up to the m -th nearest neighbors. In momentum space, this Hamiltonian is expanded as

$$H(k, t) = \langle k | H(t) | k \rangle = \sum_{m=-l}^l \sum_{\alpha, \beta} H_{m, \alpha, 0, \beta}(t) |\alpha\rangle \langle \beta| e^{-ikm}, \quad (9)$$

where the momentum eigenstate is defined as $|k\rangle = \frac{1}{\sqrt{N}} \sum_n e^{-ikn} |n\rangle$. The instantaneous eigensolutions of $H(k, t)$ at time t are given by

$$\begin{aligned}H(k, t) |u_p^R(k, t)\rangle &= E_p(k, t) |u_p^R(k, t)\rangle, \\ \langle u_p^L(k, t) | H(k, t) &= \langle u_p^L(k, t) | E_p(k, t).\end{aligned}\quad (10)$$

The Wannier state at band p is defined as

$$|w_p(n, t)\rangle = \frac{1}{\sqrt{N}} \sum_k |u_p^R(k, t)\rangle \otimes |k\rangle e^{ikn}. \quad (11)$$

For simplicity in normalizing coefficients in the formulas, we define the instantaneous eigenbasis to be biorthogonal while keeping the right eigenvectors normalized to unit norm:

$$\langle u_p^R | u_q^R \rangle = 1, \quad \langle u_q^L | u_p^R \rangle = \delta_{pq}. \quad (12)$$

Considering an adiabatic dynamic process initialized with the instantaneous Wannier state at time $t = 0$, we have the ansatz for the wave function as

$$|\psi(t)\rangle = \frac{1}{\sqrt{N}} \sum_k W_p(k, t) |u_p^R(k, t)\rangle \otimes |k\rangle e^{ikn}, \quad (13)$$

where the superposition weight satisfies $|W_p(k, 0)| = 1$, thus $|\psi(0)\rangle = |w_p(n, 0)\rangle$, with n being the initial Wannier state's center index. Under the adiabatic assumption, the wave function remains within the initially occupied energy band throughout the evolution. For simplicity, we omit the band index p in the following.

The time-dependent Hamiltonian is driven periodically, with the modulation being sufficiently slow to satisfy the adiabatic condition [42]. Due to the non-Hermitian nature of the system, the evolution is not necessarily unitary, leading to the failure of the expectation value $\langle \psi(t) | \hat{x} | \psi(t) \rangle$ to accurately represent the mass center of the wave function. To address this, wave function renormalization at each moment t is required. The renormalized average displacement over a single modulation period T is defined as

$$\Delta x^{re} = \int_0^T dt \, \partial_t \left(\frac{\langle \psi(t) | \hat{x} | \psi(t) \rangle}{\langle \psi(t) | \psi(t) \rangle} \right), \quad (14)$$

where the position operator defined as $\hat{x} = \sum_n n|n\rangle\langle n|$. Through derivations (see details in Appendix A), we express the renormalized displacement as

$$\Delta x^{re} = \iint_{\Omega} \frac{dkdt}{2\pi} \left\{ |W|^2 B^{RR} + |W|^2 \partial_k \varepsilon + |W|^2 2\text{Im}[\varepsilon] \int_0^t (\partial_k \varepsilon + B^{RR}) d\tau \right\}, \quad (15)$$

where the integration domain Ω spans the 2D Brillouin zone in momentum and time. The Berry connection are defined as $A_m^{LR}(k, t) = i\langle u^L(k, t) | \partial_m u^R(k, t) \rangle$ and $A_m^{RR}(k, t) = i\langle u^R(k, t) | \partial_m u^R(k, t) \rangle$, $m = k, t$. The Berry curvature are given by $B^{RR}(k, t) = \partial_t A_k^{RR}(k, t) - \partial_k A_t^{RR}(k, t)$ and $B^{LR}(k, t) = \partial_t A_k^{LR}(k, t) - \partial_k A_t^{LR}(k, t)$. The modified energy is $\varepsilon(k, t) = E(k, t) + A_t^{RR}(k, t) - A_t^{LR}(k, t)$, and the superposition weight evolves as $|W(k, t)| = \exp(\int_0^t d\tau \text{Im}[\varepsilon(k, \tau)])$, which is related to the imaginary part of the non-Hermitian Berry curvature.

$$\begin{aligned} \ln |W(k, t)| &= \int_0^t dt' \text{Im}[E(k, t')] \\ &+ \int_0^t dt' \int_0^k \frac{dk'}{2\pi} \text{Im}[B^{LR}(k', t')] \\ &- \int_0^k dk' \text{Im}[A_k^{LR}(k', t) - A_k^{LR}(k', 0)] \\ &+ \int_0^t dt' \text{Im}[A_t^{LR}(0, t')] \end{aligned} \quad (16)$$

The integrand in Eq. (15) reveals that the pumping average displacement can be decomposed into three distinct contributions. The first term, $|W|^2 B^{RR}$, resembles the contribution in the Hermitian Thouless pump but is weighted by $|W|^2$. We define the modified Chern number as

$$C' = \iint_{\Omega} \frac{dkdt}{2\pi} |W|^2 B^{RR}. \quad (17)$$

The second term, $|W|^2 \partial_k \varepsilon$, represents the group velocity associated with the modified energy ε , weighted by $|W|^2$. This contribution is denoted as the group velocity displacement as

$$D_V = \iint_{\Omega} \frac{dkdt}{2\pi} |W|^2 \partial_k \varepsilon. \quad (18)$$

The third term, $|W|^2 2\text{Im}[\varepsilon] \int_0^t (\partial_k \varepsilon + B^{RR}) d\tau$, involves a time accumulation and corresponds to a second-order contribution. This is referred as the acceleration displacement as

$$D_A = \iint_{\Omega} \frac{dkdt}{2\pi} |W|^2 2\text{Im}[\varepsilon] \int_0^t (\partial_k \varepsilon + B^{RR}) d\tau. \quad (19)$$

The total renormalized average displacement is then expressed as

$$\Delta x^{re} = C' + D_V + D_A. \quad (20)$$

This formula shows that the displacement of wave-packet mass center is composed of three parts: acceleration displacement, group velocity displacement and the modified Chern number, causing the displacement to deviate from the prediction of traditional Chern number in general non-Hermitian systems [Fig. 1(b)]. In Hermitian limit, the right-hand side

reduces to the standard Chern number $C = \iint_{\Omega} \frac{dkdt}{2\pi} B^{RR}$, with $|W(k, t)| = 1$. In this case, the group velocity contribution $D_V = \int dt \oint dk \partial_k E = 0$ vanishes due to periodicity, and the acceleration displacement D_A also disappears because the eigenenergies $E(k, t)$ are purely real ($\text{Im}[\varepsilon] = \text{Im}[E] = 0$).

The formalism presented in Eqs. (15)–(20) provides a framework for understanding how non-Hermiticity fundamentally reshapes quantum dynamics. The emergence of complex eigenenergies and the associated non-Hermitian Berry curvature gives rise to nonunitary evolution, as evidenced by $|W(k, t)| \neq 1$. Consequently, the modified Chern number C' may no longer be quantized, the group velocity drift D_V does not necessarily cancel due to the nonuniform weight by $|W|^2$, and the acceleration displacement D_A captures the accumulation effect caused by complex energy and the Berry curvature. These results provide a comprehensive formula for understanding the interplay between non-Hermiticity and topological pumping in open quantum systems.

III. CHARGE PUMPING IN GENERAL NONRECIPROCAL SYSTEMS

A. Quantized charge pumping breaking in general

We employ our theoretical framework to non-Hermitian systems exhibiting nontrivial Chern numbers, providing dynamical simulations to validate our analytical predictions. Specially, we exploit 1D Aubry-André-Harper (AAH) model, extended to include three sublattices and periodic nearest-neighbor couplings. This model can be configured to realize either trivial or nontrivial Chern numbers. Non-Hermiticity is introduced by implementing nonreciprocal couplings [see Fig. 2(a) for the scheme], which simultaneously induce NHSE. The Hamiltonian in momentum space is expressed in tight-binding form as

$$H(k, t) = \begin{pmatrix} 0 & J_1^-(t)e^{ik} & J_3^+(t)e^{-ik} \\ J_1^+(t)e^{-ik} & 0 & J_2^-(t)e^{ik} \\ J_3^-(t)e^{ik} & J_2^+(t)e^{-ik} & 0 \end{pmatrix}. \quad (21)$$

As depicted in Fig. 2(b), the time-dependent coupling coefficients are given by $J_m^{\pm} = J_0 \exp(a \pm \frac{d}{2} + b \sin(\frac{2\pi}{T}t + \alpha_m))$ for $m = 1, 2, 3$. The parameter a (b) represent the average (Floquet) amplitude, while the phase offsets are set as $\alpha_1 = \alpha_0$, $\alpha_2 = \alpha_0 + 2\pi/3$, $\alpha_3 = \alpha_0 + 4\pi/3$. The parameter d controls the strength of nonreciprocity. This construction enables the exploration of the interplay between non-Hermiticity and Chern topology in such systems. Figure 2(c) illustrates the PBC spectrum and three bands characterized by Chern numbers $C = -1, 2, -1$, respectively. The non-Hermitian adiabatic condition says [16]: $\frac{|\langle u_p^L(t) | \dot{u}_q^R(t) \rangle|}{|E_q - E_p|} \exp[-\text{Im} \int_0^t (E_p - E_q) dt] \ll 1$. Considering that there is no imaginary energy gap between the middle band and the others, the adiabatic assumption requires the modulation speed to be slow compared with the real energy gap. Taking $T = 4000$ suffices to ensure adiabatic evolution of the Wannier state of the middle band in this case. The dynamics of an initial Wannier state in the middle band is chosen for simulation and compared with analytical predictions, showing

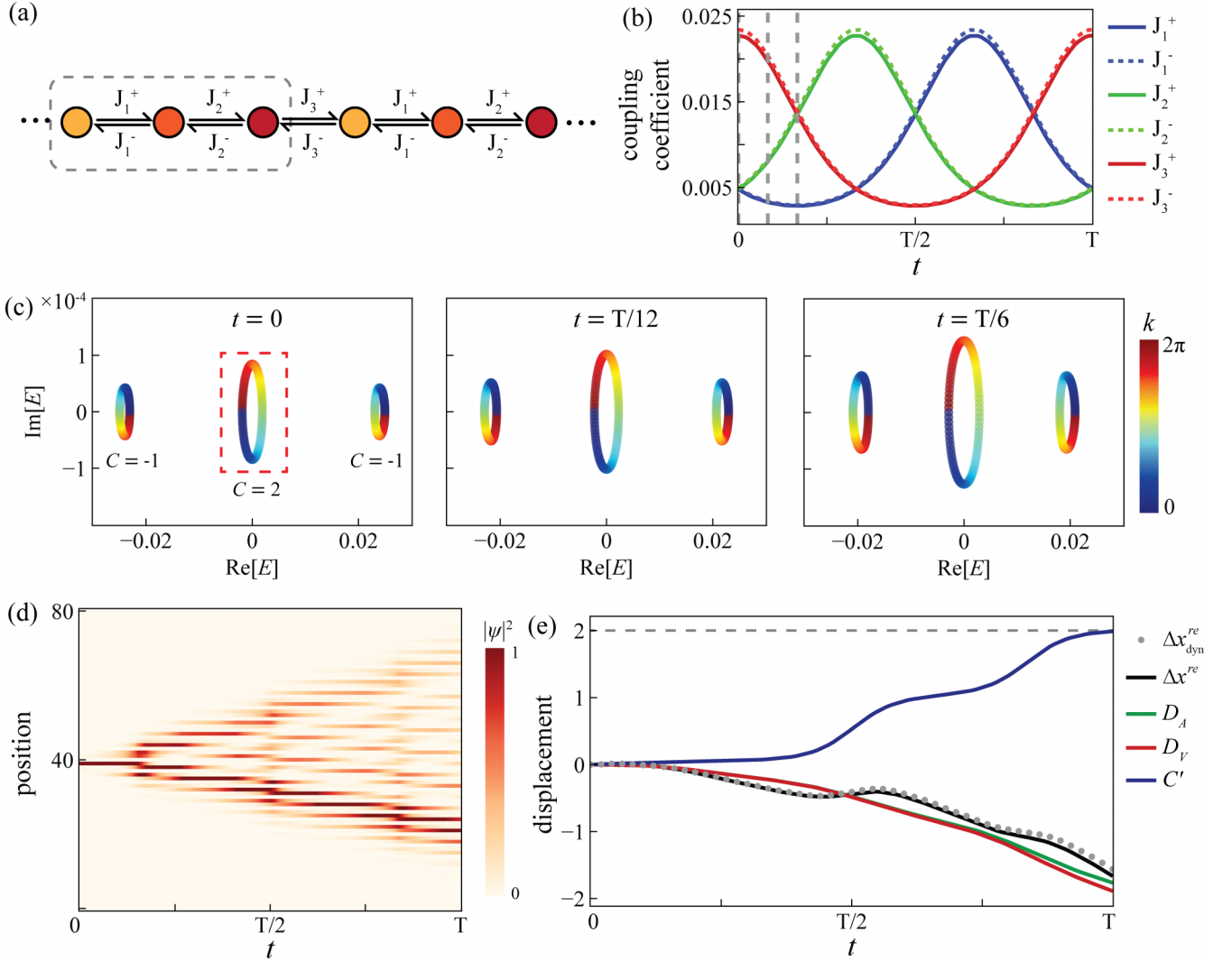


FIG. 2. Description and results of nonreciprocal AAH model. (a) The schematic of tight-binding model with nonreciprocal nearest-neighbor coupling. (b) Parameter modulation of coupling strength in single period. (c) Instantaneous spectrum under periodic boundary condition at time $t = 0$, $t = T/12$, $t = T/6$, corresponding to the gray dash lines in Fig. 2(b), respectively. Red dash square denoting the occupied band of initial Wannier state. (d) Dynamics of wave function, with initial Wannier state occupying the middle band denoted by the red dash square in (c), normalized at every time moment. (e) Total displacement Δx^{re} within single period (black line), including the modified Chern number term C' (blue line), the group velocity drift D_V (red line), the acceleration drift D_A (green line), and the mass center mass of wave function $\Delta x_{\text{dyn}}^{re}$ (gray dots) using numerical calculation. Gray dash line represents the $C = 2$ for Hermitian charge pumping. The parameters are: $T = 4000$, $J_0 = 6$, $a = -0.0132$, $d = -6 \times 10^{-5}$, $b = 3\sqrt{3}/5$, $\alpha_0 = 11\pi/6$.

agreement at all times $t \in [0, T]$. The total displacement is determined by three contributions: the modified Chern number C' , the group velocity displacement D_V , and the acceleration displacement D_A , as shown in Fig. 2(e), and the numerically calculated displacement $\Delta x_{\text{dyn}}^{re}$ fits the analytical result Δx^{re} well during the pumping period. Notably, C' remains close to the quantized Chern number $C = 2$, accurately reflecting the Wannier center motion governed by Berry curvature. For $d < 0$, the velocity displacement D_V and the acceleration displacement D_A provide a net drift of the mass center of wave packets toward $-\hat{x}$. Consequently, the total displacement Δx^{re} deviates from the quantized Chern number.

To investigate the origin of the deviation in quantized charge pumping induced by non-Hermiticity, we analyze all these displacement terms in momentum space, expressed as

integrals over the spectral densities across the 1D Brillouin zone: $C'(t) = \int \frac{dk}{2\pi} c'(k, t)$, $D_V(t) = \int \frac{dk}{2\pi} d_V(k, t)$, $D_A(t) = \int \frac{dk}{2\pi} d_A(k, t)$. And these spectral densities are defined below:

$$\begin{aligned}
 c'(k, t) &= \int_0^t |W|^2 B^{RR}(k, \tau) d\tau, \quad d_V(k, t) \\
 &= \int_0^t |W|^2 \partial_k \varepsilon(k, \tau) d\tau, \\
 d_A(k, t) &= \int_0^t |W|^2 2\text{Im}[\varepsilon(k, t_1)] \\
 &\quad \times \int_0^{t_1} (\partial_k \varepsilon(k, t_2) + B^{RR}(k, t_2)) dt_2 dt_1. \quad (22)
 \end{aligned}$$

Figure 3(a) depicts the spectral densities at $t = T$, and illustrates that the nonunitary superposition weight $|W(k, t)|$

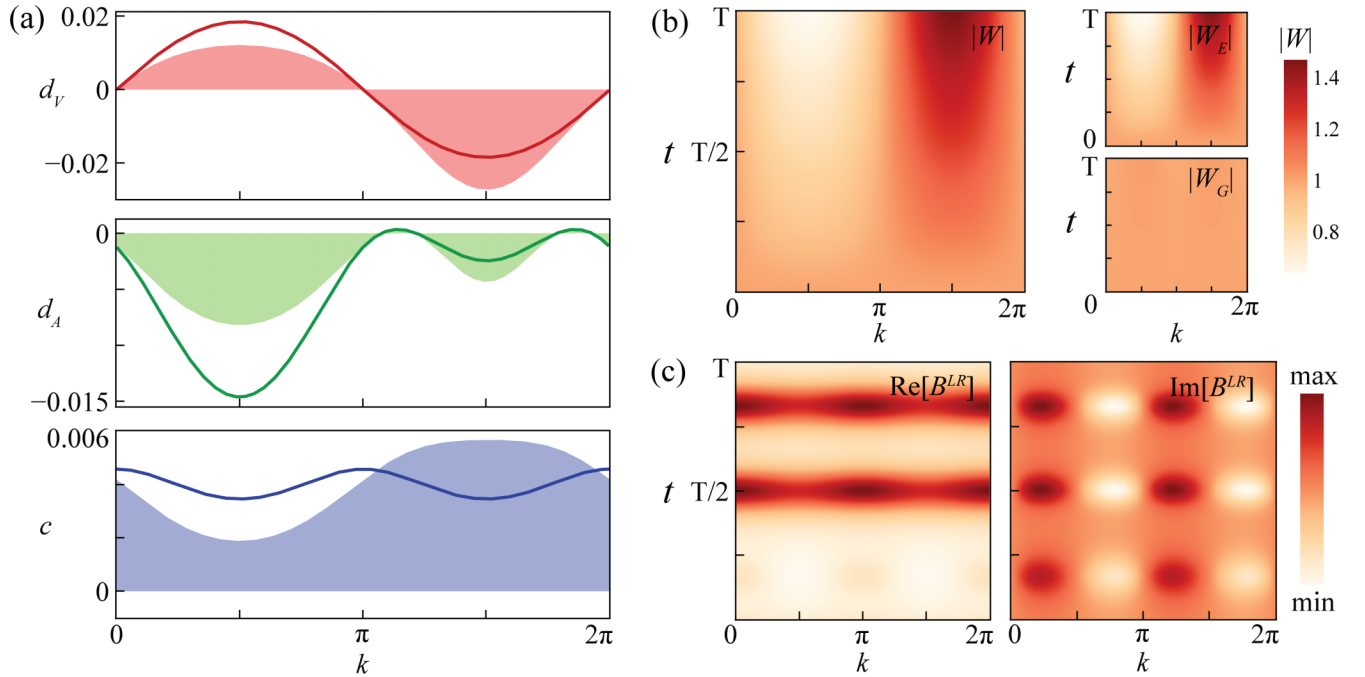


FIG. 3. Spectral densities, the superposition weight and the Berry curvature of the nonreciprocal AAH model showed in Fig. 2. (a) The spectral densities of the acceleration displacement d_v , group velocity displacement d_A and the modified Chern number c , at time $t = T$. Solid lines represent the integrands without the superposition weight, and the shading areas represent the integrands with the effect of superposition weight. (b) Superposition weight in 2D BZ. (c) Berry curvature in 2D BZ.

changes the spectral densities in general. For instance, the uneven weight alters the spectral densities of the Chern number c' , resulting in the deviation of the modified Chern number C' compared to the traditional Chern number C . Besides, without the superposition weight (solid lines), the integration of the group velocity displacement's spectral density d_v always exhibits no contribution due to periodic $\varepsilon(k, t)$ in Brillouin zone, but the weighted integration (shading area) reveals a contribution along the $-\hat{x}$ direction. This arises from the imbalanced gain and loss across different k values, resulting in a net group velocity caused by the gain-mode. The origin of $|W(k, t)|$, just as shown in Fig. 3(b), can be further understood by factorizing it into two components as

$$|W| = |W^E| \cdot |W^G|, \quad (23)$$

where the $|W^E(k, t)| = \exp(\int_0^t \text{Im}[E(k, \tau)] d\tau)$ is determined by the imaginary spectra, and the $|W^G(k, t)| = \exp(-\int_0^t \text{Im}[A_\tau^{LR}(k, \tau)] d\tau)$ stems from the imaginary part of non-Hermitian Berry connection. The PBC spectra [Fig. 2(c)] show that the negative (positive) imaginary energy mainly exhibits when $k \in [0, \pi]$ ($k \in [\pi, 2\pi]$), and thus the $|W^E|$ losses or gains in the corresponding interval of k . And the imaginary PBC spectrum dominantly influences the superposition weight through $|W^E|$ in this case. Additionally, the Berry curvature depending on k and t is also given in Fig. 3(c).

Aside from the superposition weight, non-Hermiticity directly affect the spectral density of acceleration displacement d_A , which is explained by two composed integrations in its expression. The first part, $\text{Im}[\varepsilon(k, t_1)] \int_0^{t_1} \partial_k \varepsilon(k, t_2) dt_2$, captures the accumulation contribution from the enclosed area of the modified energy ε . And the second part,

$\text{Im}[\varepsilon(k, t_1)] \int_0^{t_1} B^{RR}(k, t_2) dt_2$, represents the interference modification between spectrum and Berry curvature.

B. Initial dynamics

In 1D non-Hermitian systems, recent studies [35] on the initial dynamics of single-band lattices have revealed a self-acceleration phenomenon tied to the area enclosed by the PBC spectrum. Specifically, under the $t \rightarrow 0$ limit, the expectation value of the position operator for a single-site excitation evolves as

$$\langle x(t) \rangle \approx \frac{t^2}{\pi} \oint \text{Im}[E] \cdot d\text{Re}[E] = \frac{t^2}{\pi} A, \quad (24)$$

where A represents the area enclosed by the PBC spectrum. Our work extends this result to multi-band lattices, initializing with localized Wannier states. By expanding the dynamics up to second-order in time in the $t \rightarrow 0$ limit of Eq. (15), we obtain the equation below:

$$\begin{aligned} \Delta x^{re} = & \frac{t}{2\pi} \left[\oint dk B^{RR} \right]_{t=0} + \frac{t^2}{4\pi} \left[\oint dk \partial_t B^{RR} \right]_{t=0} \\ & + \frac{t^2}{\pi} \left[\oint d\text{Re}[\varepsilon] \cdot \text{Im}[\varepsilon] \right]_{t=0} \\ & + \frac{t^2}{\pi} \left[\oint dk \text{Im}[\varepsilon] \cdot B^{RR} \right]_{t=0}. \end{aligned} \quad (25)$$

The first two terms correspond to the velocity and acceleration arising from the motion of the Wannier center, while the third term captures the contribution of the NHSE to the acceleration. Notably, the final term demonstrates that

the cross-integration of the complex spectrum and the Berry curvature also play a significant role in the self-acceleration mechanism.

IV. RESTORE QUANTIZED CHARGE PUMPING WITH NON-HERMITICITY

A. Conditions to restore quantized charge pumping

The discussion above highlights that non-Hermiticity disrupts the quantized charge pumping determined by the Chern number. In this section, we establish the conditions under which non-Hermitian charge pumping can be restored to the quantized value dictated by the Chern number. Here, we define the displacement relative to the Chern number accumulated over one Floquet period T as

$$\Delta_T \equiv \Delta x^{re} - C = C' - C + D_V + D_A. \quad (26)$$

Through algebraic manipulations (see Appendix B), Eq. (26) can be rewritten to

$$\Delta_T = \oint \frac{dk}{2\pi} \left[(e^{2\text{Im}[Z]} - 1) \int_0^T dt B^{RR} \right] + \oint d\text{Re}Z \cdot e^{2\text{Im}[Z]}, \quad (27)$$

where $Z(k) = \int_0^T dt \varepsilon(k, t)$. Introducing a coordinate transformation along the imaginary axis in the complex plane: $\text{Im}[Z] \rightarrow \text{Im}[\tilde{Z}] = e^{2\text{Im}[Z]} - 1$, $\tilde{Z} = \text{Re}[Z] + i(e^{2\text{Im}[Z]} - 1)$, and defining $b(k) = \int_0^T dt B^{RR}(k, t)$, $F(k) = F(0) + \int_0^k dk' b(k')$, we obtain

$$\Delta_T = \int d(\text{Re}[\tilde{Z}] + F) \cdot \text{Im}[\tilde{Z}]. \quad (28)$$

Moreover, to restore non-Hermitian charge pumping to Chern number after M periods propagation, it requires the condition $\lim_{M \rightarrow \infty} \frac{\Delta_{M,T}}{M} = 0$. It is equivalent to

$$\lim_{M \rightarrow \infty} \int d(\text{Re}[Z] + F) \cdot \text{Im}[\tilde{Z}_M] = 0, \quad (29)$$

where $\text{Im}[\tilde{Z}_M] = e^{2M \cdot \text{Im}[Z]} - 1$ and $F(2\pi) - F(0) = C$. The restoration condition requires the area integration in Eq. (29) vanish. As $M \rightarrow \infty$, $\text{Im}[\tilde{Z}_M]$ converges to either ∞ or 0 due to the exponential transformation. This leads to distinct criteria depending on the behavior of $\text{Re}[Z] + F$. We, therefore, analyze the restoration condition in two cases: trivial and nontrivial.

In the topologically trivial case ($C = 0$), as k traverses from 0 to 2π , $F(k)$ forms a closed loop, leading to $\Delta_{M,T} = M \oint d(\text{Re}[Z] + F) \cdot \text{Im}[\tilde{Z}_M]$. Then, the requirement leads to

$$\lim_{M \rightarrow \infty} \oint d(\text{Re}[Z] + F) \cdot \text{Im}[\tilde{Z}_M] = 0. \quad (30)$$

A straightforward approach to satisfy this condition is by setting $\text{Im}[Z] = 0$, which ensures that the average of the modified energy $\varepsilon(k, t)$ across single period is pure real. If $\lim_{M \rightarrow \infty} \text{Im}[\tilde{Z}_M] \rightarrow \infty$, the alternative requirement becomes $F(k) = -\text{Re}[Z(k)]$. This implies that the trajectory of $F(k)$ cancels out the $\text{Re}[Z(k)]$ over the Brillouin zone.

For topologically nontrivial case, the loop of $F(k)$ cannot close at $k = 0$ because $F(2\pi) - F(0) = C \neq 0$. Consequently, the restoration condition $\text{Re}[Z(k)] + F(k)$

in Eq. (30) cannot form a closed loop. This makes the criterion $F(k) = -\text{Re}[Z(k)]$ unachievable. The only viable solution is to impose $\text{Im}[Z] = 0$. Specifically, the condition $F(k) = -\text{Re}[Z(k)]$ imposes a strict constraint on the band structure: $\int_0^T dt \text{Re}[\varepsilon(k, t)] + \int_0^k dk' \int_0^T dt B^{RR}(k', t) = \text{const}$. This constraint is challenging to realize in concrete models. However, satisfying the condition $\text{Im}[Z(k)] = 0$ is relatively straightforward. This condition implies: $\int_0^T dt \text{Im}[E - A_t^L] = 0$. Given $\int_0^T dt \text{Re}[\langle u^L(k, t) | \partial_t | u^R(k, t) \rangle] = 0$, it leads to $\int_0^T dt \text{Im}[E(k, t)] = 0$. In the section below, we provide two practical cases that satisfy this condition with different methods. The first case utilizes that pseudo-Hermitian (PH) systems possess purely real spectra, leading to the restoration naturally. The second way is choosing a proper time-variant nonreciprocal strength to make the time averages of $\text{Im}[E(k, t)]$ vanishing for every k .

B. Examples of quantized charge pumping restoration

First, we present a toy model inspired by the pseudo-Hermitian modified Qi-Wu-Zhang (MQWZ) model [43], representing a 1D time-driven lattice with long-range coupling, as shown in Fig. 4(a). The Bloch Hamiltonian is given by

$$H(k, t) = \begin{pmatrix} K_1(\delta_d(t) - \cos k) & q(\sin k + \delta_o(t)) \\ q^{-1}(\sin k - \delta_o(t)) & -K_2(\delta_d(t) - \cos k) \end{pmatrix}, \quad (31)$$

where $K_1 = \frac{2q}{q+1/q}$, $K_2 = \frac{2/q}{q+1/q}$, $\delta_d(t) = m - \cos \omega t$ and $\delta_o(t) = -i \sin \omega t$. And the coupling coefficients are depicted in Fig. 4(b). The parameter q characterizes the non-Hermitian strength, with $q = 1$ ($q \neq 1$) corresponding to Hermitian (non-Hermitian) behavior. The topological phase transition is controlled by the effective mass m , where $|m| < 2$ ($|m| > 2$) corresponds to a Chern number $C = \text{sgn}(m)$ ($C = 0$) at lower band. Choosing $m = 1$ and $q = 1.1$, the system is PT symmetric and hosts nontrivial Chern numbers [see the first row of PBC spectrum in Fig. 4(c)]. Starting with a uniformly populated lower band, both dynamic and analytical results confirm that the charge pumping over a single period is restored exactly to the Chern number, as shown in the left panel of Fig. 4(d).

The mechanism of quantized charge pumping in pseudo-Hermitian systems fundamentally differs from that in Hermitian systems. While the imbalance superposition weight persists in the PH case, it originates from the imaginary Berry curvature. Notably, the modified Chern number deviates from the quantized Chern number, but this deviation is compensated by the group velocity and acceleration displacement terms, ensuring that the total pumping displacement equals the Chern number. This restoration is protected by the implicit criteria in Eq. (29), where pseudo-Hermiticity guarantees $\text{Im}[Z(k)] = 0$ in this case.

Followingly, when the criteria in Eq. (29) are violated, the quantized charge pumping deviates. Introduce a constant on-site gain and loss on the sublattice, and the PT symmetry breaks. Thereby it violates the condition $\text{Im}[Z(k)] = 0$ in general. The modified Hamiltonian is given by

$$H'(k, t) = H(k, t) + i\gamma \sigma_z. \quad (32)$$

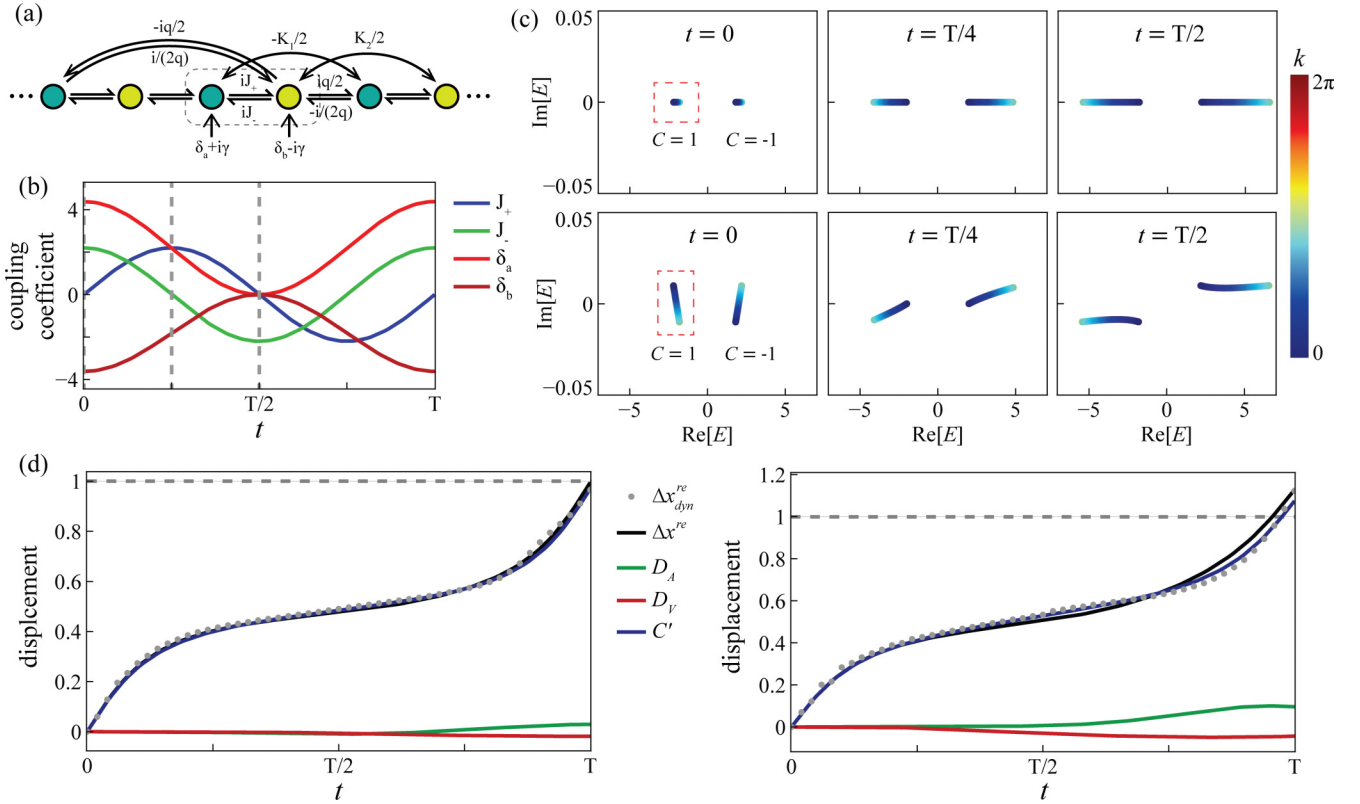


FIG. 4. Description and results in 1D MQWZ models. (a) The description of the tight-binding model with nonreciprocal long-range coupling. (b) Parameter modulation in a single period, with $T = 95$. (c) instantaneous spectrum under periodic boundary condition at time $t = 0$, $t = T/4$, $t = T/2$, corresponding to the gray dash lines in (b), respectively. Upper panels correspond to $\gamma = 0$ case, and lower panels correspond to $\gamma = 0.01$ case. Red dash square denoting the occupied band of initial Wannier state. (d) Total displacement within single period (black line), including the modified Chern number (blue line), the group velocity displacement (red line), the acceleration displacement (green line), and the mass center of wave function (gray dots). The gray dash line represents the traditional Chern number. Left panel represents to the $\gamma = 0$ case, and right panel represents to the $\gamma = 0.01$ case.

This introduces an imaginary component in the PBC spectrum, as shown in the second row of Fig. 4(c). As expected, the right panel in Fig. 4(d) shows a deviation of the charge pumping from the quantized value associated with the Chern number. Additionally, the detailed values of spectral density, superposition weight and the Berry curvature are showed in Fig. 5.

Furthermore, systems possessing NHSE can also satisfy quantized restoration, and one can exploit the non-Hermitian AAH model [Fig. 2(a)] with time-variant nonreciprocal strength $d(t)$. For instance, let $d(t) = d \cdot \sin(\omega t + \alpha_0)$, as shown in Fig. 6(a). The imaginary spectrum in the first half of the period, $t \in [0, T/2]$, and that in the second half, $t \in [T/2, T]$, cancel each other [Fig. 6(b)], ensuring that the

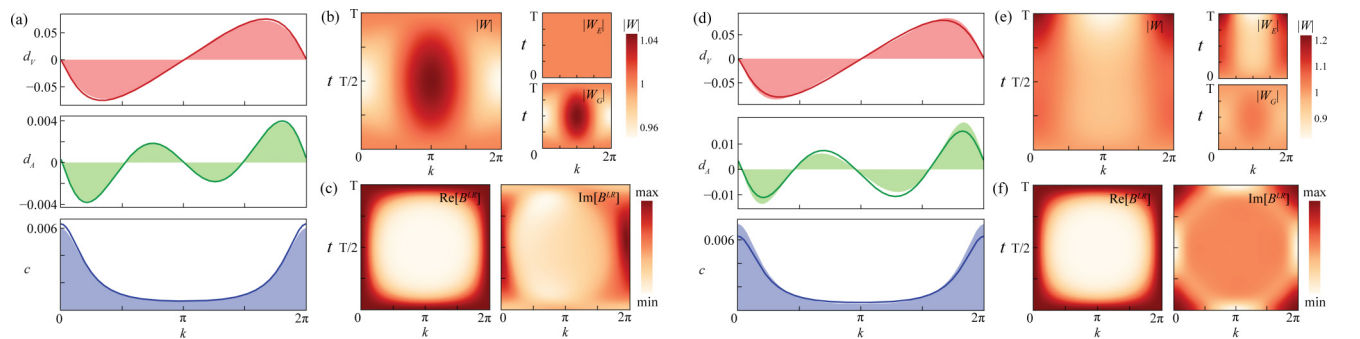


FIG. 5. Spectral densities, the superposition weight and the Berry curvatures in 1D MQWZ model corresponding to Fig. 4. (a), (d) The spectral densities of the acceleration displacement, group velocity displacement and the modified Chern number. Solid lines represent the integrand without the superposition weight, and the shading areas represent the integrand with effect of superposition weight, at time $t = T$. (b), (e) Superposition weight in 2D BZ. (c), (f) Berry curvature in 2D BZ. Figs. (a)–(c) corresponding to the case $\gamma = 0$, and (d)–(f) corresponding to the case $\gamma = 0.01$.

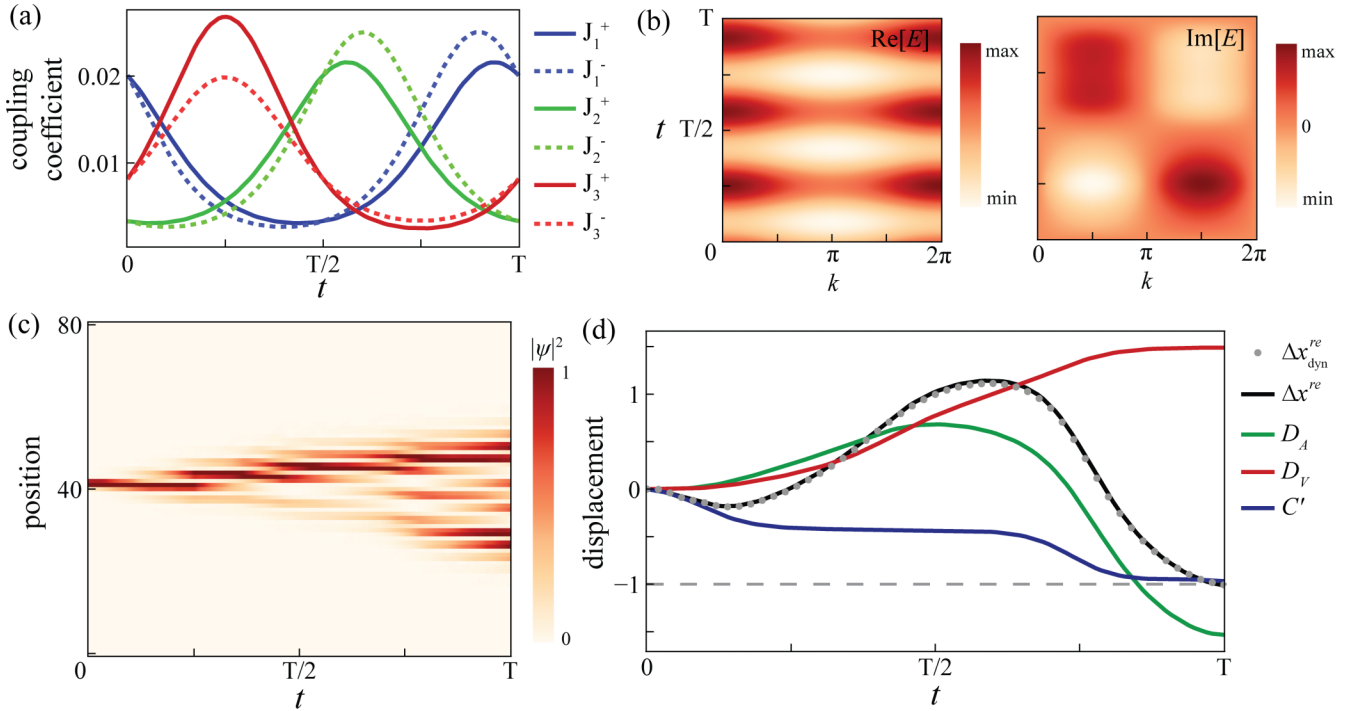


FIG. 6. Description and results of AAH model with time-variant nonreciprocal strength. (a) Parameter modulation of coupling strength in single period. (b) The PBC eigen energy of lower band with Chern number -1 . (c) Dynamics of wave function, with initial Wannier state occupying the lower band. (d) Total displacement Δx^{re} within single period (black line), including the modified Chern number term C' (blue line), the group velocity drift D_V (red line), the acceleration drift D_A (green line), and the mass center mass of wave function $\Delta x_{\text{dyn}}^{\text{re}}$ (gray dots) using numerical calculation. The gray dash line represents the traditional Chern number. The values of parameters are the same in Fig. 2.

restoration condition $\int_0^T dt \text{Im}[E(k, t)] = 0$ is satisfied. The evolution results are shown in Figs. 6(c) and 6(d), where the displacement is restored to the traditional Chern number accordingly. This result shows that even systems that possess NHSE during evolution can restore the quantized Thouless pumping by engineering the skin direction and strength to match the condition $\int_0^T dt \text{Im}[E(k, t)] = 0$ specifically.

V. CONCLUSIONS

We systematically investigated charge pumping in non-Hermitian lattices and demonstrated that non-Hermiticity fundamentally alters the topological transport behavior traditionally governed by the Chern number. Specially, we decomposed the total pumping displacement into three distinct contributions: (i) a modified Chern number reflecting Wannier center motion via the weighted Berry curvature integral, (ii) a group velocity dominated by gain-favored modes, and (iii) an acceleration linked to the enclosed area of the modified complex spectrum and its interference with the Berry curvature. These findings were validated through detailed simulations of the dynamical behavior of Wannier states in nonreciprocal AAH and MQWZ models, confirming the universality of our framework. Furthermore, we have established a precise criterion under which non-Hermitian charge pumping can exhibit quantize behavior. This criterion corresponds to the vanishing of the average imaginary spectrum. Explicit examples based on pseudo-Hermitian systems and non-Hermitian AAH model with time-variant nonreciprocal strength clearly fulfill this criterion, demonstrating its validity.

Given the generality of our theoretical approach, experimental verification should be feasible across various platforms, including ultracold atoms and photonic lattices. Notably, since the observables are naturally defined on right-eigenvector bases, quantized pumping may be directly detected through the probability distribution of Wannier state during non-Hermitian quantum walk experiments. Notably, recent studies shows that the evolution time of TP can be shortened by engineering the quantum metric [14]. Additionally, a dispersion-suppression protocol can reduce the lattice size [44,45]. Experimental realization can be further well-controlled when we provide general methods to manipulate the non-Hermitian effect. Our work renders robust theoretical results for understanding topological transport in non-Hermitian systems and opens promising avenues for future exploration, such as extensions to interacting systems and higher dimensions.

ACKNOWLEDGMENTS

This work was financially supported by National Key Research and Development Program of China (Grant No. 2023YFB2805700), the National Natural Science Foundation of China (Grants No. 12174187, No. 62288101, No. 92163216, No. 92150302, No. 92463308, No. 12174072, and No. 2021hwyq05), the Natural Science Foundation of Jiangsu Province, China (Grants No. BK20240164 and No. BK20243009) and the Fundamental Research Fund for the Central Universities, China (Grant No. 2024300329).

DATA AVAILABILITY

The data that support the findings of this article are not publicly available. The data are available from the authors upon reasonable request.

APPENDIX A: DERIVATION OF EQ. (15)

The derivation of Eq. (15) starts with the evolved wavefunction with initial Wannier state.

We have the localized Wannier state defined as

$$|w(n, t)\rangle = \sum_k |u_\mu^R(k, t)\rangle |k\rangle e^{ikn}. \quad (\text{A1})$$

Without loss of generality, one can always absorb the relative phase for each k into the gauge of eigenstates $|u_\mu^R\rangle$. The wave function satisfies $|\psi(t=0)\rangle = |w(n, 0)\rangle$. And the adiabatic assumption says

$$|\psi(t)\rangle = \sum_k W(k, t) |u_\mu^R(k, t)\rangle |k\rangle e^{ikn}. \quad (\text{A2})$$

The superposition weight $W(k, t)$ can be obtained by substitute the wave function into the Schrodinger equation and one can get

$$\begin{aligned} W(k, t) &= e^{-i \int_0^t E(k, \tau) d\tau} e^{i\gamma(k, t)}, \quad \gamma(k, t) \\ &= \int_0^t i \langle u^L(k, t) | \partial_\tau | u^R(k, t) \rangle d\tau. \end{aligned} \quad (\text{A3})$$

First, the position displacement without renormalization for single period says

$$\begin{aligned} \Delta x &= \int_0^T \partial_t \langle \psi(t) | \hat{x} | \psi(t) \rangle dt \\ &= \int_0^{2\pi} \frac{dk}{2\pi} \int_0^T \partial_t [W^*(k, t) \langle u^R(k, t) | i \partial_k (W(k, t) \\ &\quad \times |u^R(k, t)\rangle)] dt. \end{aligned} \quad (\text{A4})$$

And we define the non-Hermitian Berry connection using the bi-orthogonal basis:

$$\Gamma_k^{RR}(k, t) = i \langle u^R(k, t) | \partial_k | u^R(k, t) \rangle, \quad (\text{A5.1})$$

$$\Gamma_t^{RR}(k, t) = i \langle u^R(k, t) | \partial_t | u^R(k, t) \rangle, \quad (\text{A5.2})$$

$$\Gamma_k^{LR}(k, t) = i \langle u^L(k, t) | \partial_k | u^R(k, t) \rangle, \quad (\text{A5.3})$$

$$\Gamma_t^{LR}(k, t) = i \langle u^L(k, t) | \partial_t | u^R(k, t) \rangle, \quad (\text{A5.4})$$

$$\Delta \Gamma_t(k, t) = \Gamma_t^{RR}(k, t) - \Gamma_t^{LR}(k, t). \quad (\text{A5.5})$$

The partial derivatives of superposition weight say

$$\partial_t W(k, t) = -i(E(k, t) - \Gamma_t^{LR}(k, t))W(k, t), \quad (\text{A6.1})$$

$$\partial_t W^*(k, t) = i(E^*(k, t) - \Gamma_t^{LR*}(k, t))W^*(k, t), \quad (\text{A6.2})$$

$$\partial_k W(k, t) = iW(k, t) \int_0^t (-\partial_k E(k, \tau) + \partial_k \Gamma_\tau^{LR}(k, \tau)) d\tau. \quad (\text{A6.3})$$

The integrand in Eq. (A3) can be separated into two terms:

$$\partial_t [W^* \langle u^R | i \partial_k (W | u^R) \rangle] = \partial_t (W^* \Gamma_k^{RR} W) + i \partial_t (W^* \partial_k W). \quad (\text{A7})$$

The first term is

$$\begin{aligned} \partial_t (W^* \Gamma_k^{RR} W) &= i(E^* - \Gamma_t^{LR*}) \Gamma_k^{RR} |W|^2 + |W|^2 \partial_t \Gamma_k^{RR} \\ &\quad - i(E - \Gamma_t^{LR}) \Gamma_k^{RR} |W|^2 \\ &= 2(\text{Im}[E] - \text{Im}[\Gamma_t^{LR}]) \Gamma_k^{RR} |W|^2 \\ &\quad + |W|^2 \partial_t \Gamma_k^{RR}. \end{aligned} \quad (\text{A8})$$

And the second term says

$$\begin{aligned} i \partial_t (W^* \partial_k W) &= 2i(\text{Im}[E] - \text{Im}[\Gamma_t^{LR}]) W^* \partial_k W \\ &\quad + |W|^2 \partial_k E - |W|^2 \partial_k \Gamma_t^{LR}. \end{aligned} \quad (\text{A9})$$

With the relation $\Gamma_k^{RR}(k, t) = \Gamma_k^{RR}(k, 0) + \int_0^t d\tau \partial_\tau \Gamma_k^{RR}(k, \tau)$, one can arrive at

$$\begin{aligned} \Delta x &= \int_0^{2\pi} \frac{dk}{2\pi} \int_0^T \left[2(\text{Im}[E] - \text{Im}[\Gamma_t^{LR}]) \left(\Gamma_k^{RR}(t=0) + \int_0^t (\partial_k(E + \Delta \Gamma_\tau) + B^{RR}(k, \tau)) d\tau \right) |W|^2 \right. \\ &\quad \left. + |W|^2 \partial_k(E + \Delta \Gamma_t) + |W|^2 B^{RR}(k, t) \right] dt. \end{aligned} \quad (\text{A10})$$

And the non-Hermitian Berry curvature defined on bi-orthogonal basis says

$$B^{RR}(k, t) = \partial_t \Gamma_k^{RR} - \partial_k \Gamma_t^{RR}, \quad (\text{A11.1})$$

$$B^{LR}(k, t) = \partial_t \Gamma_k^{LR} - \partial_k \Gamma_t^{LR}. \quad (\text{A11.2})$$

Furthermore, considering that $\text{Im}[\Gamma_t^{RR}] = 0$, and defining the modified energy as $\varepsilon(k, t) = E(k, t) + \Delta \Gamma_t(k, t)$, the position displacement above can be simplified into

$$\Delta x = \int_0^{2\pi} \frac{dk}{2\pi} \int_0^T \left[2\text{Im}[\varepsilon] \left(\Gamma_k^{RR}(t=0) + \int_0^t (\partial_k \varepsilon(k, \tau) + B^{RR}(k, \tau)) d\tau \right) |W|^2 + |W|^2 (\partial_k \varepsilon(k, t) + B^{RR}(k, t)) \right] dt. \quad (\text{A12})$$

Next, the renormalized position shift is defined as

$$\Delta x^{re} = \int_0^T dt \partial_t \left(\frac{\langle \psi(t) | \hat{x} | \psi(t) \rangle}{\langle \psi(t) | \psi(t) \rangle} \right). \quad (\text{A13})$$

Considering

$$\partial_t \left(\frac{1}{\langle \psi(t) | \psi(t) \rangle} \right) = \frac{1}{\int_0^{2\pi} \frac{dk}{2\pi} |W|^2} \left(\frac{-\int_0^{2\pi} |W|^2 2\text{Im}[\varepsilon] \frac{dk}{2\pi}}{\int_0^{2\pi} \frac{dk}{2\pi} |W|^2} \right) \quad (\text{A14})$$

and

$$\begin{aligned} \langle \psi(t) | \hat{x} | \psi(t) \rangle &= \int_0^{2\pi} \frac{dk}{2\pi} W^* \langle u^R | i\partial_k (W | u^R) \rangle = \int_0^{2\pi} \frac{dk}{2\pi} (|W|^2 \Gamma_k^{RR} + iW^* \partial_k W) \\ &= \int_0^{2\pi} \frac{dk}{2\pi} \left[\Gamma_k^{RR}(t=0) + \int_0^t (\partial_k \varepsilon(k, \tau) + B^{RR}(k, \tau)) d\tau \right], \end{aligned} \quad (\text{A15})$$

the integrand in Eq. (A13) can be simplified into

$$\begin{aligned} \Delta x^{re} &= \frac{|W|^2}{\int_0^{2\pi} \frac{dk}{2\pi} |W|^2} \left\{ 2\text{Im}[\varepsilon] \left(\Gamma_k^{RR}(t=0) + \int_0^t (\partial_k \varepsilon + B^{RR}) d\tau \right) + (\partial_k \varepsilon + B^{RR}) \right. \\ &\quad \left. - \frac{\int_0^{2\pi} \frac{dk}{2\pi} |W|^2 2\text{Im}[\varepsilon]}{\int_0^{2\pi} \frac{dk}{2\pi} |W|^2} \left(\Gamma_k^{RR}(t=0) + \int_0^t (\partial_k \varepsilon + B^{RR}) d\tau \right) \right\} \\ &= \frac{|W|^2}{\int_0^{2\pi} \frac{dk}{2\pi} |W|^2} \left\{ \left(\Gamma_k^{RR}(t=0) + \int_0^t (\partial_k \varepsilon + B^{RR}) d\tau \right) \left[\frac{\partial_t |W|^2}{|W|^2} - \frac{\int_0^{2\pi} \frac{dk}{2\pi} \partial_t |W|^2}{\int_0^{2\pi} \frac{dk}{2\pi} |W|^2} \right] + (\partial_k \varepsilon + B^{RR}) \right\}. \end{aligned} \quad (\text{A16})$$

The renormalized expectation of position operator has no relation to the intensity of the state among propagation, and one can shift the Hamiltonian with a universal on-site energy without affect the Δx^{re} :

$$H'(t) = H(t) + i\eta(t). \quad (\text{A17})$$

Let $\eta(t) = -\frac{\int dk \text{Im}[\varepsilon] |W|^2}{\int dk |W|^2}$, and the corresponding quantities defined on $H'(t)$ has

$$\varepsilon'(k, t) = \varepsilon(k, t) + i\eta(t), \quad (\text{A18.1})$$

$$\int_0^{2\pi} dk \partial_t |W'|^2 = 0, \quad \int_0^{2\pi} \frac{dk}{2\pi} |W'|^2 = 1. \quad (\text{A18.2})$$

After replacing all the quantities defined on the shifted Hamiltonian in the expressions of Δx^{re} , and ignoring the prime symbol for simplicity, one can arrive at

$$\Delta x^{re} = \int_0^{2\pi} \int_0^T \frac{dk dt}{2\pi} \left\{ 2\text{Im}[\varepsilon] |W|^2 \left(\Gamma_k^{RR}(t=0) + \int_0^t (\partial_k \varepsilon + B^{RR}) d\tau \right) + |W|^2 (\partial_k \varepsilon + B^{RR}) \right\}. \quad (\text{A19})$$

From Eq. (A19), the integrand term $\Gamma_k^{RR}(t=0)$ is related to the initial gauge of the eigenbasis we chose. One can perform a k -dependent gauge transformation on the eigenbasis as

$$|u^R(k, t)\rangle \rightarrow e^{i\alpha(k)} |u^R(k, t)\rangle, \quad \langle u^L(k, t)| \rightarrow e^{-i\alpha(k)} \langle u^L(k, t)|. \quad (\text{A20})$$

And the initial Berry connection $\Gamma_k^{RR}(t=0)$ will change to $\Gamma_k^{RR}(t=0) - \partial_k \alpha(k)$. This term is related to the initial position of Wannier state $\langle \psi(0) | \hat{x} | \psi(0) \rangle$. One can choose the gauge $\alpha(k)$ by letting $\partial_k \alpha(k) = \Gamma_k^{RR}(t=0)$ to eliminate this term from the integrand.

Provided the specified gauge, we have Eq. (15) in the main text as

$$\Delta x^{re} = \int_0^{2\pi} \int_0^T \frac{dk dt}{2\pi} \left\{ 2\text{Im}[\varepsilon] |W|^2 \int_0^t (\partial_k \varepsilon + B^{RR}) d\tau + |W|^2 (\partial_k \varepsilon + B^{RR}) \right\}. \quad (\text{A21})$$

APPENDIX B: DERIVATION OF EQ. (27)

With the helper function $Y(t) = \int_0^t dt (\partial_k \varepsilon + B^{RR})$, we have

$$\int_0^T dt 2\text{Im}[\varepsilon] |W|^2 \int_0^t d\tau (\partial_k \varepsilon + B^{RR}) = \int_0^T dt (Y(t) \partial_t |W|^2) = |W(k, T)|^2 Y(T) - \int_0^T dt |W|^2 (\partial_k \varepsilon + B^{RR}), \quad (\text{B1})$$

and Eq. (15) can be simplified into

$$\Delta x^{re} = \int_0^{2\pi} \frac{dk}{2\pi} e^{\int_0^T dt 2\text{Im}[\varepsilon]} \int_0^T dt (\partial_k \varepsilon + B^{RR}) = \oint \frac{dk}{2\pi} \left[e^{\int_0^T dt 2\text{Im}[\varepsilon]} \int_0^T dt B^{RR} \right] + \oint \frac{dk}{2\pi} \left[e^{\int_0^T dt 2\text{Im}[\varepsilon]} \int_0^T dt \partial_k \varepsilon \right]. \quad (\text{B2})$$

The integration loop refers to the path along 1D BZ in momentum space. Using the definition of $Z(k)$ in the main text, the second term in Eq. (B2) becomes

$$\begin{aligned} \oint \frac{dk}{2\pi} e^{\int_0^T dt 2\text{Im}[Z]} \int_0^T dt \partial_k \varepsilon &= i \oint \frac{dk}{2\pi} e^{2\text{Im}[Z]} \partial_k \text{Im}[Z] + \oint \frac{dk}{2\pi} e^{2\text{Im}[Z]} \partial_k \text{Re}[Z] \\ &= \frac{i}{4\pi} \oint d e^{2\text{Im}[Z]} + \oint \frac{d\text{Re}[Z]}{2\pi} e^{2\text{Im}[Z]} \\ &= \oint \frac{d\text{Re}[Z]}{2\pi} e^{2\text{Im}[Z]}. \end{aligned} \quad (\text{B3})$$

Then, we have

$$\Delta x^{re} = \oint \frac{dk}{2\pi} e^{2\text{Im}[Z]} \int_0^T dt B^{RR} + \oint \frac{d\text{Re}[Z]}{2\pi} e^{2\text{Im}[Z]}. \quad (\text{B4})$$

With the definition of traditional Chern number $C = \oint \frac{dk}{2\pi} \int_0^T dt B^{RR}$, we have

$$\Delta_T = \Delta x^{re} - C = \oint \frac{dk}{2\pi} \left[(e^{2\text{Im}[Z]} - 1) \int_0^T dt B^{RR} \right] + \oint \frac{d\text{Re}[Z]}{2\pi} e^{2\text{Im}[Z]}. \quad (\text{B5})$$

-
- [1] D. J. Thouless, Quantization of particle-transport, *Phys. Rev. B* **27**, 6083 (1983).
 - [2] R. Citro and M. Aidelsburger, Thouless pumping and topology, *Nat. Rev. Phys.* **5**, 87 (2023).
 - [3] Y. K. Sun, X. L. Zhang, F. Yu, Z. N. Tian, Q. D. Chen, and H. B. Sun, Non-Abelian Thouless pumping in photonic waveguides, *Nat. Phys.* **18**, 1080 (2022).
 - [4] Y. K. Sun, Z. L. Shan, Z. N. Tian, Q. D. Chen, and X. L. Zhang, Two-dimensional non-Abelian Thouless pump, *Nat. Commun.* **15**, 9311 (2024).
 - [5] O. B. You, S. J. Liang, B. Y. Xie, W. L. Gao, W. M. Ye, J. Zhu, and S. Zhang, Observation of non-Abelian Thouless pump, *Phys. Rev. Lett.* **128**, 244302 (2022).
 - [6] A. Kapustin and L. Spodyneiko, Higher-dimensional generalizations of the Thouless charge pump, *arXiv:2003.09519*.
 - [7] T. Tuloup, R. W. Bomantara, and J. Gong, Breakdown of quantization in nonlinear Thouless pumping, *New J. Phys.* **25**, 083048 (2023).
 - [8] M. Ezawa, N. Ishida, Y. Ota, and S. Iwamoto, Nonadiabatic nonlinear non-Hermitian quantized pumping, *Phys. Rev. Res.* **6**, 033258 (2024).
 - [9] X. Z. Cao, C. Y. Jia, Y. Hu, and Z. X. Liang, Nonlinear Thouless pumping of solitons across an impurity, *Phys. Rev. A* **110**, 013305 (2024).
 - [10] M. Jrgensen, S. Mukherjee, C. Jrg, and M. C. Rechtsman, Quantized fractional Thouless pumping of solitons, *Nat. Phys.* **19**, 420 (2023).
 - [11] W. C. Ma *et al.*, Experimental observation of a generalized Thouless pump with a single spin, *Phys. Rev. Lett.* **120**, 120501 (2018).
 - [12] M. Lohse, C. Schweizer, O. Zilberberg, M. Aidelsburger, and I. Bloch, A Thouless quantum pump with ultracold bosonic atoms in an optical superlattice, *Nat. Phys.* **12**, 350 (2016).
 - [13] S. Nakajima, T. Tomita, S. Taie, T. Ichinose, H. Ozawa, L. Wang, M. Troyer, and Y. Takahashi, Topological Thouless pumping of ultracold fermions, *Nat. Phys.* **12**, 296 (2016).
 - [14] W. E. Song *et al.*, Fast topological pumps via quantum metric engineering on photonic chips, *Sci. Adv.* **10**, eadn5028 (2024).
 - [15] P. Wang, Q. D. Fu, R. H. Peng, Y. V. Kartashov, L. Torner, V. V. Konotop, and F. W. Ye, Two-dimensional Thouless pumping of light in photonic moiré lattices, *Nat. Commun.* **13**, 6738 (2022).
 - [16] Z. M. Zhang, T. Y. Li, X. W. Luo, and W. Yi, Biorthogonal topological charge pumping in non-Hermitian systems, *Phys. Rev. B* **109**, 224307 (2024).
 - [17] W. C. Hu, H. L. Wang, P. P. Shum, and Y. D. Chong, Exceptional points in a non-Hermitian topological pump, *Phys. Rev. B* **95**, 184306 (2017).
 - [18] K. Y. Shi, L. W. Qiao, Z. Y. Zheng, and W. Zhang, Floquet topological phases and skin effects in periodically driven non-Hermitian systems, *Phys. Rev. A* **110**, 022222 (2024).
 - [19] T. Ozawa and H. Schomerus, Geometric contribution to adiabatic amplification in non-Hermitian systems, *Phys. Rev. Res.* **7**, 013173 (2025).
 - [20] S. Yao, F. Song, and Z. Wang, Non-Hermitian Chern bands, *Phys. Rev. Lett.* **121**, 136802 (2018).
 - [21] S. Longhi, Non-Hermitian dynamical topological winding in photonic mesh lattices, *Opt. Lett.* **49**, 3672 (2024).
 - [22] B. A. Bhargava, I. C. Fulga, J. van den Brink, and A. G. Moghaddam, Non-Hermitian skin effect of dislocations and its topological origin, *Phys. Rev. B* **104**, L241402 (2021).
 - [23] K. Ding, C. Fang, and G. C. Ma, Non-Hermitian topology and exceptional-point geometries, *Nat. Rev. Phys.* **4**, 745 (2022).
 - [24] V. Mittal, A. Raj, S. Dey, and S. K. Goyal, Persistence of topological phases in non-Hermitian quantum walks, *Sci. Rep.* **11**, 10262 (2021).
 - [25] K. Zhang, Z. S. Yang, and C. Fang, Correspondence between winding numbers and skin modes in non-Hermitian systems, *Phys. Rev. Lett.* **125**, 126402 (2020).
 - [26] S. Y. Yao and Z. Wang, Edge states and topological invariants of non-Hermitian systems, *Phys. Rev. Lett.* **121**, 086803 (2018).
 - [27] Z. S. Yang, K. Zhang, C. Fang, and J. P. Hu, Non-Hermitian bulk-boundary correspondence and auxiliary generalized Brillouin zone theory, *Phys. Rev. Lett.* **125**, 226402 (2020).
 - [28] L. Xiao, T. S. Deng, K. K. Wang, G. Y. Zhu, Z. Wang, W. Yi, and P. Xue, Non-Hermitian bulk-boundary correspondence in quantum dynamics, *Nat. Phys.* **16**, 761 (2020).

- [29] N. Hatano and H. Obuse, Delocalization of a non-Hermitian quantum walk on random media in one dimension, *Ann. Phys. (NY)* **435**, 168615 (2021).
- [30] Y. O. Nakai, N. Okuma, D. Nakamura, K. Shimomura, and M. Sato, Topological enhancement of nonnormality in non-Hermitian skin effects, *Phys. Rev. B* **109**, 144203 (2024).
- [31] M. Gao, C. Sheng, Y. Zhao, R. He, L. Lu, W. Chen, K. Ding, S. Zhu, and H. Liu, Quantum walks of correlated photons in non-Hermitian photonic lattices, *Phys. Rev. B* **110**, 094308 (2024).
- [32] T. Li, J.-Z. Sun, Y.-S. Zhang, and W. Yi, Non-Bloch quench dynamics, *Phys. Rev. Res.* **3**, 023022 (2021).
- [33] W.-T. Xue, Y.-M. Hu, F. Song, and Z. Wang, Non-Hermitian edge burst, *Phys. Rev. Lett.* **128**, 120401 (2022).
- [34] L. Xiao, W. T. Xue, F. Song, Y. M. Hu, W. Yi, Z. Wang, and P. Xue, Observation of non-Hermitian edge burst in quantum dynamics, *Phys. Rev. Lett.* **133**, 070801 (2024).
- [35] S. Longhi, Non-Hermitian skin effect and self-acceleration, *Phys. Rev. B* **105**, 245143 (2022).
- [36] P. Xue, Q. Lin, K. K. Wang, L. Xiao, S. Longhi, and W. Yi, Self acceleration from spectral geometry in dissipative quantum-walk dynamics, *Nat. Commun.* **15**, 4381 (2024).
- [37] H. Ghaemi-Dizicheh and H. Schomerus, Compatibility of transport effects in non-Hermitian nonreciprocal systems, *Phys. Rev. A* **104**, 023515 (2021).
- [38] B. Mera and T. Ozawa, Kahler geometry and Chern insulators: Relations between topology and the quantum metric, *Phys. Rev. B* **104**, 045104 (2021).
- [39] C. C. Ye, W. L. Vleeshouwers, S. Heatley, V. Gritsev, and C. M. Smith, Quantum metric of non-Hermitian Su-Schrieffer-Heeger systems, *Phys. Rev. Res.* **6**, 023202 (2024).
- [40] D. D. Solnyshkov, C. Leblanc, L. Bessonart, A. Nalitov, J. H. Ren, Q. Liao, F. Li, and G. Malpuech, Quantum metric and wave packets at exceptional points in non-Hermitian systems, *Phys. Rev. B* **103**, 125302 (2021).
- [41] J. F. Ren, J. Li, H. T. Ding, and D. W. Zhang, Identifying non-Hermitian critical points with the quantum metric, *Phys. Rev. A* **110**, 052203 (2024).
- [42] P. Weinberg, M. Bukov, L. D'Alessio, A. Polkovnikov, S. Vajna, and M. Kolodrubetz, Adiabatic perturbation theory and geometry of periodically-driven systems, *Phys. Rep.* **688**, 1 (2017).
- [43] M. Karami, E. Sadeghi, and P. Zamani, Band topology and symmetry in pseudo-Hermitian systems, *Phys. E* **160**, 115941 (2024).
- [44] S. Hu, Y. Ke, Y. Deng, and C. Lee, Dispersion-suppressed topological Thouless pumping, *Phys. Rev. B* **100**, 064302 (2019).
- [45] S. Hu, Y. Ke, and C. Lee, Topological quantum transport and spatial entanglement distribution via a disordered bulk channel, *Phys. Rev. A* **101**, 052323 (2020).